Remote Detection

DOI: 10.1002/anie.201100965

Ultrafast Microscopy of Microfluidics: Compressed Sensing and Remote Detection

*Eva Paciok and Bernhard Blümich**

compressed sensing · microfluidics · microscopy · NMR spectroscopy · velocimetry

The vast amount of progress made in microfluidic technology during the past 20 years has brought forth a variety of ingenious miniaturized lab-on-a-chip devices with a broad range of applications, from simple mixing in chemical syntheses to advanced microbiological incubation and medical diagnostics.[1,2] One persistent issue in the design and online monitoring of microfluidic processes is the lack of a fast but precise, non-invasive detection method that unifies imaging, velocimetry, molecular sensing, and chemical spectroscopy, with universal adaptability to the various kinds of microfluidic applications. NMR spectroscopy is renowned for its unmatched potential to non-invasively reveal and correlate spatial and spectroscopic information in a large variety of chemical systems. This versatility makes NMR the method of choice for microfluidic analytics. However, the extremely low signal intensity derived from microscopic sample volumes has imposed restrictions on the spectral, spatial, and temporal resolution of microfluidic NMR.[3] Microfluidic NMR has so far focused on either spectroscopy or imaging, and thus has failed to live up to its full potential for universal microanalysis.

Recent developments in NMR methodology, including probe miniaturization,[4] hyperpolarization,[5] and remote detection[6] have achieved a remarkable gain in sensitivity along with a drastic reduction of the measurement time.[7] Moreover, current approaches to combine these methods on microfluidic platforms have yielded very promising spectroscopic and velocimetric results in investigations of microfluidic liquid–liquid mixing,[8] and even enabled imaging of gaseous flow in microfluidic structures.[9,10] Now, Bajaj et al.[11] have succeeded in demonstrating another remarkable gain in sensitivity by combining compressed sensing[12] with remote detection for NMR monitoring of microfluidics by imaging and velocity mapping. The cumulated sensitivity gain of six orders of magnitude suggests NMR will become a standard method for lab-on-a-chip processes.

Although rich in information, the signal sensitivity of NMR is low, as only a few nuclei contribute to the magnetization in thermodynamic equilibrium. The low sensitivity of NMR is typically overcome by signal averaging at the expense of measurement time, and the obtained information is averaged over the entire measurement period. If samples are dilute or microscopic, measurement noise becomes even more of an issue, as it derives from the whole detection volume. When imaging and analyzing fluids in the narrow channels of a microfluidic chip by standard NMR, the noise is collected from the entire volume of the chip. The straightforward way to minimize the noise is to match the detection volume to the sample volume and to place microcoils into the various channels of the chip. This approach complicates chip design enormously and draws the attention away from the "big picture" of all the locations in the chip to a few preselected ones.

To maintain both the big picture of full-volume excitation and the sensitivity of microcoil detection, one can take advantage of the fluid motion to locally separate signal detection from signal excitation and encoding. This principle of remote detection is depicted in Figure 1. The detection noise is reduced to that of the fluid volume by detecting the fluid with a microcoil at the outlet of the chip, where it is confined to a small volume, while encoding the spatial information earlier, when the fluid is distributed across the various channels of the chip. This approach leads to a sensitivity gain with an associated decrease of measurement time by three to four orders of magnitude, so that even gas flow in microchannels can be imaged (Figure 2). Another

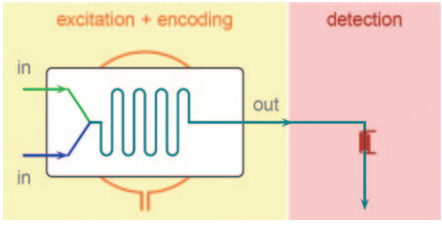

Figure 1. Schematic diagram of a remote detection setup for microfluidic chips. Full-volume excitation with a large radiofrequency coil is followed by ultrasensitive detection in a microscopic volume. This eliminates the trade-off between field of view and signal-to-noise of conventional NMR experiments with only one coil for excitation and detection.

[*] Dipl.-Chem. E. Paciok, Prof. Dr. B. Blümich
Institute for Technical and Macromolecular Chemistry
RWTH Aachen
52056 Aachen (Germany)
Fax: (+49) 24-80-22185
E-mail: bbluemich@mc.rwth-aachen.de
Homepage: http://www.mc.rwth-aachen.de

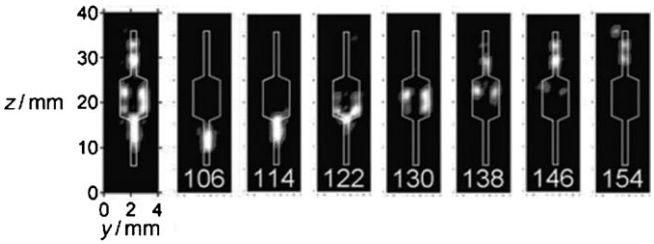

Figure 2. Spin-density images of hyperpolarized propane flowing through a microfluidic device. The individual images represent time-of-flight reconstructions at different points in time after excitation (t in ms). The sum of all the images is shown on the left. Reproduced from Ref. [10].

remarkable advantage of remote detection is that spectra and images can be acquired at very high flow rates. As a result, repetition times between excitation experiments are not dictated by the T_1 relaxation of the investigated compound, but by the rate with which the excited volume is replaced by fresh fluid. Considering most organic compounds have long T_1 relaxation times in the range of several seconds, remote detection can reduce measurement times by one or two orders of magnitude.

However, Bajaj et al. moved yet another step further in accelerating the time for imaging the flow inside microfluidic devices by making use of the sparse distribution of channels inside the chip. Just as sparse electronic data sets are nowadays routinely compressed for storage, the NMR data of a sparsely populated image can be sampled and compressed following the principles of compressed sensing. Bajaj et al. used wavelet transformations and nonlinear reconstruction to gain another factor of two to three orders of magnitude in shortening the measurement time. This is an astonishing leap for NMR towards high-resolution on-line monitoring in microfluidic devices. Moreover, and in contrast to all optical monitoring techniques for microfluidics, the setup requires neither transparent samples nor confocal arrangements, and is therefore not restricted to specific systems or simplified model setups.

Experimental proof of these concepts is given with an analysis of the flow patterns in a capillary, a microfluidic serpentine mixer, and a constricted capillary. A time resolution of 30 ms and a spatial resolution of better than 15 μm was achieved, with flow rates approaching 1 m s^{-1}. Separate images are obtained for the spatial distribution of fluids which share common velocity ranges, and thus a similar time of flight. The information for each image is acquired at a different time at the output, following the initial procedure for spatial encoding of all components in the device. The fast components arrive at the detector first and the slower ones later. The measured data correlate the two complementary descriptions of flow—the Lagrangian and the Laplacian views—where the flow field is characterized either in terms of fluid parcel trajectories and times of flight, or in terms of the velocity vector in each pixel, respectively. They can be processed into a multitude of high-resolution maps that depict spatial, velocimetric, and chemical distributions of fluids, as shown in Figures 3 and 4, or rendered into movies, which visualize the flow process through the microfluidic structure.

However, there are also limitations to the method. The time delay between excitation and detection makes it vulnerable to fast T_1 relaxation and changes in flow dynamics

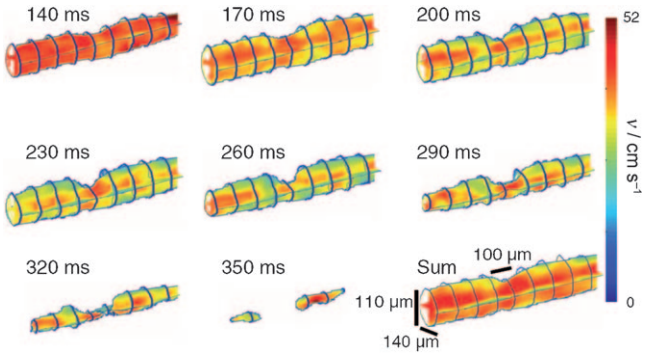

Figure 3. Highly resolved three-dimensional velocity maps of fast flow in a microcapillary with a constriction. The time-of-flight reconstruction yields images with a temporal resolution of 30 ms. Reproduced from Ref. [11].

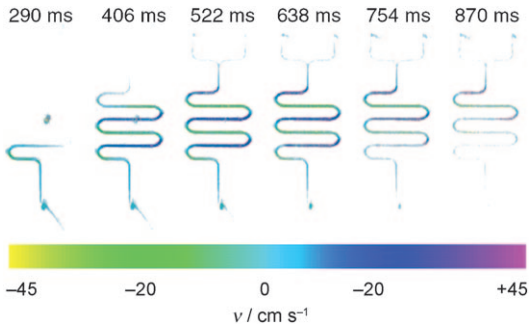

Figure 4. Highly resolved two-dimensional velocity maps of fast flow inside a serpentine micromixer. The individual images represent time-of-flight reconstructions at different points in time after excitation. Reproduced from Ref. [11].

after encoding, with the first leading to signal attenuation and information loss,[13] and the latter to falsified time-of-flight reconstruction. Both can, in principle, be minimized with careful experimental design, by ensuring detection before relaxation by using short transport distances and fast flow, as well as plug-flow conditions in the outlet tubing. Furthermore, it has been shown that the encoded chemical or physical information can be preserved regardless of T_1 relaxation, by storing it in a long-lived spin state, which relaxes over periods much longer than the T_1 value[14] so that remote detection may be extended to microfluidic setups with low flow rates or prepolarization setups with long transport distances.

Moreover, different techniques to polarize the nuclear magnetization to values much higher than those attained in thermodynamic equilibrium are emerging[7] together with novel methods for sensitive detection by using microfabricated magnetometers.[15–17] As a result, and despite the limitations imposed by Boltzmann's law of thermodynamic

equilibrium, NMR spectroscopy as a tool to probe the function of microfluidic devices is expected to have a significant impact on moving laboratory-scale experiments to the chip and on advancing studies of cellular chemistry, metabolomics, and high-throughput screening in combinatorial chemistry. In combination with low-field NMR spectroscopy, even personalized microanalytical systems come within reach.

Received: February 8, 2011
Published online: April 28, 2011

[1] For an introduction into microfluidic technology, see G. M. Whitesides, *Nature* **2006**, *442*, 368 – 373.
[2] For recent reviews of microfluidic technology, see a) A. B. Theberge, F. Courtois, Y. Schaerli, M. Fischlechner, C. Abell, F. Hollfelder, W. T. S. Huck, *Angew. Chem.* **2010**, *122*, 5982 – 6005; *Angew. Chem. Int. Ed.* **2010**, *49*, 5846 – 5868; b) A. Abou-Hassan, O. Sandre, V. Cabuil, *Angew. Chem.* **2010**, *122*, 6408 – 6428; *Angew. Chem. Int. Ed.* **2010**, *49*, 6268 – 6286; c) V. Kumar, M. Paraschivoiu, K. D. P. Nigam, *Chem. Eng. Sci.* **2011**, *66*, 1329 – 1373; d) G. S. Jeong, S. Chung, C.-B. Kim, S.-H. Lee, *Analyst* **2010**, *135*, 460 – 473; e) P. Tabeling, *Lab Chip* **2009**, *9*, 2428 – 2436.
[3] For a minireview of NMR spectroscopy in microfluidics, see E. Harel, *Lab Chip* **2009**, *9*, 17 – 23.
[4] For recent achievements in the miniaturization of NMR probes, see a) J. Bart, H. J. W. G. Janssen, J. P. J. M. van Bentum, A. P. M. Kentgens, H. J. G. E. Gardeniers, *J. Magn. Reson.* **2009**, *201*, 175 – 185; b) J. Bart, A. J. Kolkman, A. J. Oosthoek-de Vries, K. Koch, P. J. Nieuwland, H. J. W. G. Janssen, J. P. J. M. van Bentum, K. A. M. Ampt, F. P. J. T. Rutjes, S. S. Wijmenga, H. J. G. E. Gardeniers, A. P. M. Kentgens, *J. Am. Chem. Soc.* **2009**, *131*, 5014 – 5015; c) A. V. Demyanenko, L. Zhao, Y. Kee, S. Nie, S. E. Fraser, J. M. Tyszka, *J. Magn. Reson.* **2009**, *200*, 38 – 48; d) J. Anders, G. Chiaramonte, P. SanGiorgio, G. Boero, *J. Magn. Reson.* **2009**, *201*, 239 – 249.
[5] For detailed reviews of hyperpolarization in NMR spectroscopy, see a) J. Natterer, J. Bargon, *Prog. Nucl. Magn. Reson. Spectrosc.* **1997**, *31*, 293 – 315; b) T. G. Walker, W. Happer, *Rev. Mod. Phys.* **1997**, *69*, 629 – 642; c) K. Golman, L. E. Olsson, O. Axelsson, S. Mansson, M. Karlsson, J. S. Petersson, *Br. J. Radiol.* **2003**, *76*, S118 – S127.
[6] Remote detection: A. J. Moulé, M. M. Spence, S.-I. Han, J. A. Seeley, K. L. Pierce, S. Saxena, A. Pines, *Proc. Natl. Acad. Sci. USA* **2003**, *100*, 9122 – 9127.
[7] For a recent Highlight, see H. W. Spiess, *Angew. Chem.* **2008**, *120*, 649 – 652; *Angew. Chem. Int. Ed.* **2008**, *47*, 639 – 642.
[8] E. Harel, A. Pines, *J. Magn. Reson.* **2008**, *193*, 199 – 206.
[9] C. Hilty, E. E. McDonell, J. Granwehr, K. L. Pierce, S.-I. Han, A. Pines, *Proc. Natl. Acad. Sci. USA* **2005**, *102*, 14960 – 14963.
[10] V.-V. Telkki, V. V. Zhivonitko, S. Ahola, K. V. Kovtunov, J. Jokisaari, I. V. Koptyug, *Angew. Chem.* **2010**, *122*, 8541 – 8544; *Angew. Chem. Int. Ed.* **2010**, *49*, 8363 – 8366.
[11] V. S. Bajaj, J. Paulsen, E. Harel, A. Pines, *Science* **2010**, *330*, 1078 – 1081.
[12] Compressed sensing: a) M. Lustig, D. L. Donoho, J. M. Santos, J. M. Pauly, *IEEE SignalProcess. Mag.* **2008**, *25*, 72 – 82; b) D. J. Holland, D. M. Malioutov, A. Blake, A. J. Sederman, L. F. Gladden, *J. Magn. Reson.* **2010**, *203*, 236 – 246; c) J. Paulsen, V. S. Bajaj, A. Pines, *J. Magn. Reson.* **2010**, *205*, 196 – 201.
[13] For a thorough discussion of remote detection sensitivity, see J. Granwehr, J. A. Seeley, *J. Magn. Reson.* **2006**, *179*, 280 – 289.
[14] R. Sarkar, P. R. Vasos, G. Bodenhausen, *J. Am. Chem. Soc.* **2007**, *129*, 328 – 334.
[15] For a review of optical magnetometry, see D. Budker, M. Romalis, *Nat. Phys.* **2007**, *3*, 227 – 234.
[16] M. P. Ledbetter, I. M. Savukov, D. Budker, V. Shah, S. Knappe, J. Kitching, D. J. Michalak, S. Xu, A. Pines, *Proc. Natl. Acad. Sci. USA.* **2008**, *105*, 2286 – 2290.
[17] J. M. Taylor, P. Cappellaro, L. Childress, L. Jiang, D. Budker, P. R. Hemmer, A. Yacoby, R. Walsworth, M. D. Ludkin, *Nat. Phys.* **2008**, *4*, 810 – 816.

